

$\mathcal{O}(a^2)$ corrections to the one-loop propagator and bilinears of
clover fermions with Symanzik improved gluons

M. Constantinou^a, V. Lubicz^b, H. Panagopoulos^a, F. Stylianos^a

^a *Department of Physics, University of Cyprus,
P.O.Box 20537, Nicosia CY-1678, Cyprus*

^b*Dipartimento di Fisica, Università di Roma Tre and INFN,
Sezione di Roma Tre, Via della Vasca Navale 84, I-00146 Roma, Italy*
*email: marthac@ucy.ac.cy, lubicz@fis.uniroma3.it,
haris@ucy.ac.cy, fstyli01@ucy.ac.cy*

Abstract

We calculate corrections to the fermion propagator and to the Green's functions of all fermion bilinear operators of the form $\bar{\Psi}\Gamma\Psi$, to one-loop in perturbation theory.

We employ the Wilson/clover action for fermions and the Symanzik improved action for gluons.

The novel aspect of our calculations is that they are carried out to second order in the lattice spacing, $\mathcal{O}(a^2)$. Consequently, they have addressed a number of new issues, most notably the appearance of loop integrands with strong IR divergences (convergent only beyond 6 dimensions). Such integrands are not present in $\mathcal{O}(a^1)$ improvement calculations; there, IR divergent terms are seen to have the same structure as in the $\mathcal{O}(a^0)$ case, by virtue of parity under integration, and they can thus be handled by well-known techniques. We explain how to correctly extract the full $\mathcal{O}(a^2)$ dependence; in fact, our method is generalizable to any order in a .

The $\mathcal{O}(a^2)$ corrections to the quark propagator and Green's functions computed in this paper are useful to improve the nonperturbative RI-MOM determination of renormalization constants for quark bilinear operators.

Our results depend on a large number of parameters: coupling constant, number of colors, lattice spacing, external momentum, clover parameter, Symanzik coefficients, gauge parameter. To make these results most easily accessible to the reader, we have included them in the distribution package of this paper, as an ASCII file named: `Oa2results.m`; the file is best perused as Mathematica input.

PACS numbers: 11.15.Ha, 12.38.Gc, 11.10.Gh, 12.38.Bx

Keywords: Lattice QCD, Lattice perturbation theory, Fermion propagator, Fermion bilinears, Improved actions

I. INTRODUCTION

A major issue facing Lattice Gauge Theory, since its early days, has been the reduction of effects which are due to the finite lattice spacing a , in order to better approach the elusive continuum limit. A systematic framework to address this issue is Symanzik's program [1], in which the regularized action is improved through a judicious inclusion of irrelevant operators with increasing dimensionality. Thus far, most efforts have been directed towards $\mathcal{O}(a^1)$ improvement; this is automatic in some cases (i.e. requires no tuning of parameters), by symmetry considerations alone. Such is the case, for example, of the twisted mass formulation of QCD [2, 3] at maximal twist, where certain observables are $\mathcal{O}(a^1)$ improved, as a consequence of symmetries of the fermion action: Setting the maximal twist requires the tuning of only a single parameter in the action, i.e. the critical quark mass, and no further improvement of the operators is required.

In other cases, such as with the clover fermion action, $\mathcal{O}(a)$ corrections must be also implemented on individual operators; such corrections take the form of an additional, finite (non UV-divergent) renormalization or an admixture of appropriate higher dimensional operators. Determining the values of the renormalization functions or mixing coefficients requires an evaluation of appropriate Green's functions, as dictated by the choice of renormalization scheme; these Green's functions can be evaluated perturbatively or nonperturbatively.

As regards the perturbative evaluation of Green's functions for the "ultralocal" fermion bilinear operators $O_a^\Gamma = \bar{\Psi}\lambda_a\Gamma\Psi$ (Γ denotes all possible distinct products of Dirac matrices, and λ_a is a flavor symmetry generator) and the related fermion propagator, the following types of calculations have appeared thus far in the literature: (i) One-loop calculations to $\mathcal{O}(a^0, \ln a)$ have been performed in the past several years for a wide variety of actions, ranging from Wilson fermions/gluons to overlap fermions and Symanzik gluons [4, 5, 6, 7, 8, 9, 10]. (ii) There exist one-loop computations of $\mathcal{O}(a^1)$ corrections, with an arbitrary fermion mass [6, 11]. (iii) The first two-loop calculations of Green's functions for O_a^Γ were completed recently, to $\mathcal{O}(a^0)$, for Wilson/clover/twisted-mass fermions and Wilson gluons [12, 13]. (iv) A number of $\mathcal{O}(a^0)$ results have also been obtained by means of stochastic perturbation theory [14, 15, 16].

One-loop computations of $\mathcal{O}(a^2)$ corrections did not exist to date; indeed they present some novel difficulties, as compared to $\mathcal{O}(a^1)$. Extending $\mathcal{O}(a^0)$ calculations up to $\mathcal{O}(a^1)$

does not bring in any novel types of singularities: For instance, terms which were convergent to $\mathcal{O}(a^0)$ may now develop at worst an infrared (IR) logarithmic singularity in 4 dimensions and the way to treat such singularities is well known; also, in most of the cases, e.g. for $m = 0$, terms which were already IR divergent to $\mathcal{O}(a^0)$ will not contribute to $\mathcal{O}(a^1)$, by parity of loop integration. On the contrary, many IR singularities encountered at $\mathcal{O}(a^2)$ would persist even up to 6 dimensions, making their extraction more delicate. In addition to that, there appear Lorentz non-invariant contributions in $\mathcal{O}(a^2)$ terms, such as $\sum_{\mu} p_{\mu}^4/p^2$ (p : external momentum).

In this paper we present a one-loop perturbative calculation, to $\mathcal{O}(a^2)$, of the quantum corrections to the fermion propagator and to the complete basis of local fermion bilinear currents $\bar{\Psi}\Gamma\Psi$, using massless fermions described by the Wilson/clover action. We use a 3-parameter family of Symanzik improved gluon actions, comprising all cases which are in common use (Wilson, tree-level Symanzik, Iwasaki [17], DBW2 [18], Lüscher-Weisz [19, 20]). All calculations have been performed for generic values of the gauge parameter. Also, by virtue of working in a massless scheme, all of our results are applicable to other ultralocal fermion actions as well, such as the twisted mass or Osterwalder-Seiler action [21]. Our results can be used to construct $\mathcal{O}(a^2)$ improved definitions of the fermion bilinears. In particular, they will be used in Ref. [22] to improve the nonperturbative determinations, with the RI-MOM method [23], of renormalization constants of bilinear quark operators.

This paper is organized as follows: Section II is an outline of our calculational procedure; Section III describes in detail the evaluation of a prototype IR divergent integral; Sections IV and V present the corrections to the propagator and to fermion bilinears, respectively; Section VI contains a discussion and concluding remarks. Appendix A contains a basis of the divergent integrals which appear in the calculation, evaluated to the required order in a .

II. DESCRIPTION OF THE CALCULATION

Our calculation makes use of the clover (SW) action for fermions; for N_f flavor species this action reads, in standard notation,

$$\begin{aligned}
S_F = & \sum_f \sum_x (4r + m_f) \bar{\psi}_f(x) \psi_f(x) \\
& - \frac{1}{2} \sum_f \sum_{x, \mu} \left[\bar{\psi}_f(x) (r - \gamma_\mu) U_{x, x+\mu} \psi_f(x + \mu) + \bar{\psi}_f(x + \mu) (r + \gamma_\mu) U_{x+\mu, x} \psi_f(x) \right] \\
& - \frac{1}{4} c_{\text{SW}} \sum_f \sum_{x, \mu, \nu} \bar{\psi}_f(x) \sigma_{\mu\nu} \hat{F}_{\mu\nu}(x) \psi_f(x), \tag{1}
\end{aligned}$$

The Wilson parameter r is set to $r = 1$; f is a flavor index; $\sigma_{\mu\nu} = [\gamma_\mu, \gamma_\nu]/2$; the clover coefficient c_{SW} is kept as a free parameter throughout. Powers of the lattice spacing a have been omitted and may be directly reinserted by dimensional counting. The tensor $\hat{F}_{\mu\nu}$ is a lattice representation of the gluon field tensor, defined through

$$\hat{F}_{\mu\nu} \equiv \frac{1}{8} (Q_{\mu\nu} - Q_{\nu\mu}) \tag{2}$$

where $Q_{\mu\nu}$ is the sum of the plaquette loops

$$\begin{aligned}
Q_{\mu\nu} = & U_{x, x+\mu} U_{x+\mu, x+\mu+\nu} U_{x+\mu+\nu, x+\nu} U_{x+\nu, x} + U_{x, x+\nu} U_{x+\nu, x+\nu-\mu} U_{x+\nu-\mu, x-\mu} U_{x-\mu, x} \\
& + U_{x, x-\mu} U_{x-\mu, x-\mu-\nu} U_{x-\mu-\nu, x-\nu} U_{x-\nu, x} + U_{x, x-\nu} U_{x-\nu, x-\nu+\mu} U_{x-\nu+\mu, x+\mu} U_{x+\mu, x} \tag{3}
\end{aligned}$$

We perform our calculation for mass independent renormalization schemes, so that $m_f = 0$; this simplifies the algebraic expressions, but at the same time requires special treatment when it comes to IR singularities. By taking $m_f = 0$, our calculation and results are identical also for the twisted mass action and the Osterwalder-Seiler action in the chiral limit (in the so called twisted mass basis).

For gluons we employ the Symanzik improved action, involving Wilson loops with 4 and 6 links¹, which is given by the relation

$$\begin{aligned}
S_G = & \frac{2}{g_0^2} \left[c_0 \sum_{\text{plaquette}} \text{Re Tr} \{1 - U_{\text{plaquette}}\} + c_1 \sum_{\text{rectangle}} \text{Re Tr} \{1 - U_{\text{rectangle}}\} \right. \\
& \left. + c_2 \sum_{\text{chair}} \text{Re Tr} \{1 - U_{\text{chair}}\} + c_3 \sum_{\text{parallelogram}} \text{Re Tr} \{1 - U_{\text{parallelogram}}\} \right] \tag{4}
\end{aligned}$$

¹ 1×1 *plaquette*, 1×2 *rectangle*, 1×2 *chair* (bent rectangle), and $1 \times 1 \times 1$ *parallelogram* wrapped around an elementary 3-d cube.

The coefficients c_i can in principle be chosen arbitrarily, subject to the following normalization condition, which ensures the correct classical continuum limit of the action

$$c_0 + 8c_1 + 16c_2 + 8c_3 = 1 \tag{5}$$

Some popular choices of values for c_i used in numerical simulations will be considered in this work, and are itemized in Table I; they are normally tuned in a way as to ensure $\mathcal{O}(a^2)$ improvement in the pure gluon sector. Our one-loop Feynman diagrams do not involve pure gluon vertices, and the gluon propagator depends only on three combinations of the Symanzik parameters: $C_0 \equiv c_0 + 8c_1 + 16c_2 + 8c_3 (= 1)$, $C_1 \equiv c_2 + c_3$, $C_2 \equiv c_1 - c_2 - c_3$; therefore, with no loss of generality all these sets of values have $c_2 = 0$.

For the algebraic operations involved in evaluating the Feynman diagrams relevant to this calculation, we make use of our symbolic package in Mathematica. Next, we briefly describe the required steps:

- Algebraic manipulations:

The first step in evaluating each diagram is the contraction among vertices, which is performed automatically once the algebraic expression of the vertices and the topology (“incidence matrix”) of the diagram are specified. The outcome of the contraction is a preliminary expression for the diagram; there follow simplifications of the color dependence, Dirac matrices and tensor structures. We also fully exploit symmetries of the theory (periodicity, reflection, conjugation, hypercubic, etc.) to limit the proliferation of the algebraic expressions.

- Dependence on external momentum:

Even though one-loop computations are normally a straightforward procedure, extending to $\mathcal{O}(a^2)$ introduces several complications, especially when isolating logarithms and Lorentz non-invariant terms. As a first task we want to reduce the number of infrared divergent integrals to a minimal set. To do this, we use two kinds of subtractions among the propagators,

using the simple equalities

$$\frac{1}{\tilde{q}^2} = \frac{1}{\hat{q}^2} + \left\{ \frac{4 \sum_{\mu} \sin^4(q_{\mu}/2) - 4 \left(\sum_{\mu} \sin^2(q_{\mu}/2) \right)^2}{\tilde{q}^2 \hat{q}^2} \right\} \quad (6)$$

$$\begin{aligned} D(q) &= D_{plaq}(q) + \left\{ D(q) - D_{plaq}(q) \right\} \\ &= D_{plaq}(q) + D_{plaq}(q) \left\{ D_{plaq}^{-1}(q) - D^{-1}(q) \right\} D(q) \end{aligned} \quad (7)$$

where q stands for k or $k + a p$, and k (p) is the loop (external) momentum. The denominator of the fermion propagator, \tilde{q}^2 , is defined as

$$\tilde{q}^2 = \sum_{\mu} \sin^2(q_{\mu}) + \left(m_f + \frac{r}{2} \hat{q}^2 \right)^2, \quad \hat{q}^2 = 4 \sum_{\mu} \sin^2\left(\frac{q_{\mu}}{2}\right) \quad (8)$$

For the present work, one sets $m_f = 0$ and $r = 1$, as used in Eq. (6); D is the 4×4 Symanzik gluon propagator; the expression for the matrix $(D_{plaq}^{-1}(q) - D^{-1}(q))$, which is $\mathcal{O}(q^4)$, is independent of the gauge parameter, λ , and it can be easily obtained in closed form. Moreover, we have

$$(D_{plaq}(q))_{\mu\nu} = \frac{\delta_{\mu\nu}}{\hat{q}^2} - (1 - \lambda) \frac{\hat{q}_{\mu} \hat{q}_{\nu}}{(\hat{q}^2)^2} \quad (9)$$

Terms in curly brackets of Eqs. (6) and (7) are less IR divergent than their unsubtracted counterparts, by two powers in the momentum. These subtractions are performed iteratively until all primitively divergent integrals (initially depending on the fermion and the Symanzik propagator) are expressed in terms of the Wilson gluon propagator.

Having reduced the number of distinct divergent integrals down to a minimum, the most laborious task is the computation of these integrals, which is performed in a noninteger number of dimensions $D > 4$. Ultraviolet divergences are explicitly isolated à la Zimmermann and evaluated as in the continuum. The remainders are D -dimensional, parameter-free, zero external momentum lattice integrals which can be recast in terms of Bessel functions, and finally expressed as sums of a pole part plus numerical constants. We analytically evaluate an extensive basis of superficially divergent loop integrals, listed in Eqs. (A1) - (A10) of Appendix A; a few of these were calculated in Ref. [24]. The integrals of Eqs. (A1), (A2), (A3), are the most demanding ones in the list; they must be evaluated to two further orders in a , beyond the order at which an IR divergence initially sets in. As a consequence,

their evaluation requires going to $D > 6$ dimensions. Fortunately, they are a sufficient basis for all massless integrals which can appear in any $\mathcal{O}(a^2)$ one-loop calculation; that is, any such computation can be recast in terms of (A1), (A2), (A3), plus other integrals which are more readily handled. A correct way to evaluate (A1), (A2), (A3) has not been presented previously in the literature, despite their central role in $\mathcal{O}(a^2)$ calculations, and this has prevented one-loop computations to $\mathcal{O}(a^2)$ thus far. The calculation of such an integral is given in detail in the next section.

Terms which are IR convergent can be treated by Taylor expansion in ap to the desired order. Alternatively, the extraction of the ap dependence may be performed using iteratively subtractions of the form

$$f(k + ap) = f(k) + \left[f(k + ap) - f(k) \right] \quad (10)$$

This leads to exact relations such as the following ones

$$\begin{aligned} \frac{1}{\widehat{k+ap}^2} &= \frac{1}{\tilde{k}^2} - \frac{\sum_{\mu} \sin(2k_{\mu} + ap_{\mu}) \sin(ap_{\mu})}{\widehat{k+ap}^2 \tilde{k}^2} \\ &- \frac{\sum_{\mu} \sin(k_{\mu} + \frac{ap_{\mu}}{2}) \sin(\frac{ap_{\mu}}{2}) \left(\hat{k}^2 + \widehat{k+ap}^2 \right)}{\widehat{k+ap}^2 \tilde{k}^2} \end{aligned} \quad (11)$$

$$\frac{1}{\widehat{k+ap}^2} = \frac{1}{\hat{k}^2} - \frac{4 \sum_{\mu} \sin(k_{\mu} + \frac{ap_{\mu}}{2}) \sin(\frac{ap_{\mu}}{2})}{\widehat{k+ap}^2 \hat{k}^2} \quad (12)$$

In these relations the exact ap dependence of the remainders is under full control; this type of subtraction is especially useful when applied to the Symanzik propagator.

- Numerical integration:

The required numerical integrations of the algebraic expressions for the loop integrands (a total of $\sim 40,000$ terms) are performed by highly optimized Fortran programs; these are generated by our Mathematica ‘integrator’ routine. Each integral is expressed as a sum over the discrete Brillouin zone of finite lattices, with varying size L ($4^4 \leq L^4 \leq 128^4$), and evaluated for all values of the Symanzik coefficients listed in Table I (corresponding to the Plaquette, Symanzik, Iwasaki, TILW and DBW2 action).

- Extrapolation:

The last part of the evaluation is the extrapolation of the numerical results to infinite lattice size. This procedure entails a systematic error, which is reliably estimated, using a sophisticated inference technique; for one-loop quantities we expect a fractional error smaller than 10^{-7} .

III. EVALUATION OF A PRIMITIVELY DIVERGENT INTEGRAL

Divergent integrals which appear in calculations up to $\mathcal{O}(a^1)$ may be evaluated using the standard procedure of Kawai et al. [25], in which one subtracts and adds to the original integrand its naive Taylor expansion, to the appropriate order with respect to a , in $D \rightarrow 4^+$ dimensions: The subtracted integrand, being UV convergent, is calculated in the continuum limit $a \rightarrow 0$, using the methods of Ref. [26], while the Taylor expansion terms are recast in terms of Bessel functions and are evaluated in the limit $\epsilon \rightarrow 0$ ($\epsilon \equiv (4 - D)/2$).

In contrast to the above, some of the integrals in the present work, given that they must be evaluated to $\mathcal{O}(a^2)$, have Taylor expansions which remain IR divergent all the way up to $D \leq 6$ dimensions. A related difficulty regards Kawai's procedure: Subtracting from the original integral its Taylor expansion in D -dimensions to the appropriate order, the UV-convergent subtracted expression at which one arrives can no longer be evaluated in the continuum limit by naively setting $a \rightarrow 0$, because there will be $\mathcal{O}(a^2)$ corrections which must not be neglected. These novel difficulties plague integrals A1, A2, A3, of Appendix A. Using a combination of momentum shifts, integration by parts and trigonometric identities, one may express A2 and A3 in terms of A1 and other less divergent integrals. Thus, it suffices to address the evaluation of A1

$$A1(p) = \int_{-\pi}^{\pi} \frac{d^4k}{(2\pi)^4} \frac{1}{\hat{k}^2 \overbrace{k + ap}^2} \quad (13)$$

This is a prototype case of an integral which is IR divergent in $D \leq 6$ dimensions; in fact, all other integrals encountered in the present calculation may be expressed in terms of $A1(p)$ plus other integrals which are IR convergent at $D > 4$ (and are thus amenable to a more standard treatment).

First we split the original integrand I into two parts

$$I \equiv \frac{1}{\widehat{k^2 k + ap}^2} = I_1 + I_2 \quad (14)$$

where I_2 is obtained from I by a series expansion, with respect to the arguments of all trigonometric functions, to subleading order; I_1 is simply the remainder $I - I_2$

$$\begin{aligned} I_1 = & \frac{k^2 - \frac{k^4}{12} - \hat{k}^2}{k^2 \hat{k}^2 \widehat{k + ap}^2} + \frac{k^4 (k^2 - \hat{k}^2)}{12 (k^2)^2 \hat{k}^2 \widehat{k + ap}^2} + \frac{k^4 \left((k + ap)^2 - \widehat{k + ap}^2 \right)}{12 (k^2)^2 (k + ap)^2 \widehat{k + ap}^2} \\ & + \frac{(k + ap)^2 - \frac{(k + ap)^4}{12} - \widehat{k + ap}^2}{k^2 (k + ap)^2 \widehat{k + ap}^2} + \frac{(k + ap)^4 \left((k + ap)^2 - \widehat{k + ap}^2 \right)}{12 k^2 ((k + ap)^2)^2 \widehat{k + ap}^2} \end{aligned} \quad (15)$$

$$I_2 = \frac{1}{k^2 (k + ap)^2} + \left[\frac{(k + ap)^4}{12 k^2 ((k + ap)^2)^2} + \frac{k^4}{12 (k^2)^2 (k + ap)^2} \right] \quad (16)$$

($q^4 \equiv \sum_{\mu} q_{\mu}^4$). I_2 is free of trigonometric functions, while I_1 is naively Taylor expandable to $\mathcal{O}(a^2)$; its integral equals

$$\int_{-\pi}^{\pi} \frac{d^4 k}{(2\pi)^4} I_1 = 0.004210419649(1) + a^2 p^2 0.0002770631001(3) + \mathcal{O}(a^4, a^4 \ln a) \quad (17)$$

The errors appearing in the above equation come from extrapolations to infinite lattice size.

To evaluate the integral of I_2 we split the hypercubic integration region into a sphere of arbitrary radius μ about the origin ($\mu \leq \pi$) plus the rest

$$\int_{-\pi}^{\pi} = \int_{|k| \leq \mu} + \left(\int_{-\pi}^{\pi} - \int_{|k| \leq \mu} \right) \quad (18)$$

The integral outside the sphere is free of IR divergences and is thus Taylor expandable to any order, giving² (for $\mu = 3.14155$)

$$\left(\int_{-\pi}^{\pi} - \int_{|k| \leq \mu} \right) \frac{d^4 k}{(2\pi)^4} I_2 = 6.42919(3) 10^{-3} + a^2 p^2 6.2034(1) 10^{-5} + \mathcal{O}(a^4) \quad (19)$$

We are now left with the integral of I_2 over a sphere. The most infrared divergent part of I_2 is $1/(k^2 (k + ap)^2)$, with IR degree of divergence -4, and can be integrated *exactly*, giving

$$\int_{|k| \leq \mu} \frac{d^4 k}{(2\pi)^4} \frac{1}{k^2 (k + ap)^2} = \frac{1}{16\pi^2} \left(1 - \ln\left(\frac{a^2 p^2}{\mu^2}\right) \right) \quad (20)$$

² Due to its peculiar domain, this integral has been evaluated by a Monte Carlo routine, rather than as a sum over lattice points. The errors in Eq. (19) are thus Monte Carlo errors.

The remaining two terms comprising I_2 have IR degree of divergence -2, thus their calculation to $\mathcal{O}(a^2)$ can be performed in D -dimensions, with D slightly greater than 4. Let us illustrate the procedure with one of these terms: $k^4/((k^2)^2 (k + ap)^4)$. By appropriate substitutions of

$$\frac{1}{(k + \bar{p})^2} = \frac{1}{k^2} + \frac{-2(k \cdot \bar{p}) - \bar{p}^2}{k^2 (k + \bar{p})^2} \quad (\bar{p} \equiv ap) \quad (21)$$

we split this term as follows

$$\begin{aligned} \frac{k^4}{(k^2)^2 (k + \bar{p})^2} &= \left[\frac{k^4}{(k^2)^3} + \frac{k^4 (-2(k \cdot \bar{p}) - \bar{p}^2)}{(k^2)^4} + \frac{4 k^4 (k \cdot \bar{p})^2}{(k^2)^5} \right] \\ &+ \left(\frac{k^4 (4(k \cdot \bar{p})\bar{p}^2 + (\bar{p}^2)^2)}{(k^2)^4 (k + \bar{p})^2} + \frac{4 k^4 (k \cdot \bar{p})^2 (-2(k \cdot \bar{p}) - \bar{p}^2)}{(k^2)^5 (k + \bar{p})^2} \right) \end{aligned} \quad (22)$$

The part in square brackets is polynomial in a and can be integrated easily, using D -dimensional spherical coordinates. The remaining part is UV-convergent; thus the integration domain can now be recast in the form

$$\int_{|k| \leq \mu} = \int_{|k| < \infty} - \int_{\mu \leq |k| < \infty} \quad (23)$$

The integral over the whole space can be performed using the methods of Ref. [26], whereas the integral outside the sphere of radius μ is $\mathcal{O}(a^3)$ and may be safely dropped. The same procedure is applied to the last term of I_2 . Adding the contributions from all the steps described above, we check that the result is independent of μ .

IV. CORRECTION TO THE FERMION PROPAGATOR

The fermion propagator is the most common example of an off-shell quantity suffering from $\mathcal{O}(a)$ effects. Capitani et al. [6] have calculated the first order terms in the lattice spacing for massive fermions. We carried out this calculation beyond the first order correction, taking into account all terms up to $\mathcal{O}(a^2)$. Our results, to $\mathcal{O}(a^1)$, are in perfect agreement with those of Ref. [6]. The clover coefficient c_{SW} has been considered to be a free parameter and our results are given as a polynomial of c_{SW} . Moreover, the dependence on the number of colors N , the coupling constant g and the gauge fixing parameter λ , is shown explicitly. The Symanzik coefficients, c_i , appear in a nontrivial way in the propagator and, thus, we tabulate these results for different choices of c_i .

The one-loop Feynman diagrams that enter our 2-point Green's function calculation, are illustrated in Fig. 1.



Fig. 1: One-loop diagrams contributing to the fermion propagator. Wavy (solid) lines represent gluons (fermions).

Next, we provide the total expression for the inverse fermion propagator S^{-1} as a function of g , N , c_{SW} , λ . Here we should point out that for dimensional reasons, there is a global prefactor $1/a$ multiplying our expressions for the inverse propagator, and thus, the $\mathcal{O}(a^2)$ correction is achieved by considering all terms up to $\mathcal{O}(a^3 p^3)$.

$$\begin{aligned}
S_{(p)}^{-1} &= i \not{p} + \frac{a}{2} p^2 - i \frac{a^2}{6} \not{p}^3 \\
&- i \not{p} \tilde{g}^2 \left[\varepsilon^{(0,1)} - 4.79200956(5) \lambda + \varepsilon^{(0,2)} c_{\text{SW}} + \varepsilon^{(0,3)} c_{\text{SW}}^2 + \lambda \ln(a^2 p^2) \right] \\
&- a p^2 \tilde{g}^2 \left[\varepsilon^{(1,1)} - 3.86388443(2) \lambda + \varepsilon^{(1,2)} c_{\text{SW}} + \varepsilon^{(1,3)} c_{\text{SW}}^2 - \frac{1}{2} (3 - 2 \lambda - 3 c_{\text{SW}}) \ln(a^2 p^2) \right] \\
&- i a^2 \not{p}^3 \tilde{g}^2 \left[\varepsilon^{(2,1)} + 0.507001567(9) \lambda + \varepsilon^{(2,2)} c_{\text{SW}} + \varepsilon^{(2,3)} c_{\text{SW}}^2 \right. \\
&\quad \left. + \left(\frac{101}{120} - \frac{11}{30} C_2 - \frac{\lambda}{6} \right) \ln(a^2 p^2) \right] \\
&- i a^2 p^2 \not{p} \tilde{g}^2 \left[\varepsilon^{(2,4)} + 1.51604667(9) \lambda + \varepsilon^{(2,5)} c_{\text{SW}} + \varepsilon^{(2,6)} c_{\text{SW}}^2 \right. \\
&\quad \left. + \left(\frac{59}{240} + \frac{c_1}{2} + \frac{C_2}{60} - \frac{1}{4} \left(\frac{3}{2} \lambda + c_{\text{SW}} + c_{\text{SW}}^2 \right) \right) \ln(a^2 p^2) \right] \\
&- i a^2 \not{p} \frac{\sum_{\mu} p_{\mu}^4}{p^2} \tilde{g}^2 \left[-\frac{3}{80} - \frac{C_2}{10} - \frac{5}{48} \lambda \right]
\end{aligned} \tag{24}$$

where $\tilde{g}^2 \equiv g^2 C_F / (16\pi^2)$, $C_F = (N^2 - 1) / (2N)$, $C_2 = c_1 - c_2 - c_3$, $\not{p}^3 = \sum_{\mu} \gamma_{\mu} p_{\mu}^3$, and the specific values $\lambda = 1$ (0) correspond to the Feynman (Landau) gauge. The quantities $\varepsilon^{(i,j)}$ appearing in our results for S^{-1} are numerical coefficients depending on the Symanzik parameters, calculated for each action we have considered and tabulated in Tables II - V;

the index i denotes the power of the lattice spacing a that they multiply. In all Tables, the systematic errors in parentheses come from the extrapolation over finite lattice size $L \rightarrow \infty$.

Terms proportional to $1/a$ have been left out of Eq. (24) for conciseness; such terms represent $\mathcal{O}(g^2)$ corrections to the critical value of the fermion mass.

We observe that the $\mathcal{O}(a^1)$ logarithms as well as all terms multiplied by λ , are independent of the Symanzik coefficients; on the contrary $\mathcal{O}(a^2)$ logarithms have a mild dependence on the Symanzik parameters. A number of Lorentz non-invariant tensors ($\sum_{\mu} p_{\mu}^4, \not{p}^{\beta}$) appear in $\mathcal{O}(a^2)$ correction terms, compatibly with hypercubic invariance. Finally, our $\mathcal{O}(a^1)$ results for the Plaquette action, are in agreement with Eq. (37) of Ref. [6].

To enable cross-checks and comparisons, the per-diagram contributions $d_1(p)$, $d_2(p)$ are presented below. The tadpole diagram 1 of Fig. 1 is free of logarithmic terms and independent of c_{SW} ; its final expression is

$$\begin{aligned} \frac{d_1(p)}{\tilde{g}^2} &= i \not{p} \left[\tilde{\varepsilon}_1^{(0,1)} + 3.050262540200(1) \lambda \right] + a p^2 \left[\tilde{\varepsilon}_1^{(1,1)} + 1.529131270100(1) \lambda \right] \\ &+ i a^2 \not{p}^{\beta} \left[\tilde{\varepsilon}_1^{(2,1)} - 0.509710423367(1) \lambda \right] \end{aligned} \quad (25)$$

where the numerical values for the Symanzik dependent coefficients $\tilde{\varepsilon}_1^{(i,1)}$ are listed in Table VI. The main contribution to the propagator correction comes from diagram 2, as can be seen from the following expression, with $\tilde{\varepsilon}_2^{(i,1)}$ provided in Table VII. The remaining terms with coefficients $\varepsilon^{(i,j)}$ are the same as in Eq. (24).

$$\begin{aligned} \frac{d_2(p)}{\tilde{g}^2} &= i \not{p} \left[\tilde{\varepsilon}_2^{(0,1)} - 7.850272109(6) \lambda + \varepsilon^{(0,2)} c_{\text{SW}} + \varepsilon^{(0,3)} c_{\text{SW}}^2 + \lambda \ln(a^2 p^2) \right] \\ &+ a p^2 \left[\tilde{\varepsilon}_2^{(1,1)} - 5.39301570(2) \lambda + \varepsilon^{(1,2)} c_{\text{SW}} + \varepsilon^{(1,3)} c_{\text{SW}}^2 - \frac{1}{2} (3 - 2 \lambda - 3 c_{\text{SW}}) \ln(a^2 p^2) \right] \\ &+ i a^2 \not{p}^{\beta} \left[\tilde{\varepsilon}_2^{(2,1)} + 1.016711991(9) \lambda + \varepsilon^{(2,2)} c_{\text{SW}} + \varepsilon^{(2,3)} c_{\text{SW}}^2 \right. \\ &\quad \left. + \left(\frac{101}{120} - \frac{11}{30} C_2 - \frac{\lambda}{6} \right) \ln(a^2 p^2) \right] \\ &+ i a^2 p^2 \not{p} \left[\varepsilon^{(2,4)} + 1.51604667(9) \lambda + \varepsilon^{(2,5)} c_{\text{SW}} + \varepsilon^{(2,6)} c_{\text{SW}}^2 \right. \\ &\quad \left. + \left(\frac{59}{240} + \frac{c_1}{2} + \frac{C_2}{60} - \frac{1}{4} \left(\frac{3}{2} \lambda + c_{\text{SW}} + c_{\text{SW}}^2 \right) \right) \ln(a^2 p^2) \right] \\ &+ i a^2 \not{p} \frac{\sum_{\mu} p_{\mu}^4}{p^2} \left[-\frac{3}{80} - \frac{C_2}{10} - \frac{5}{48} \lambda \right] \end{aligned} \quad (26)$$

Using our results for the fermion propagator, we can compute the multiplicative renormalization function of the quark field (Z_Ψ).

V. FERMION BILINEAR OPERATORS

In the context of this work we also study the $\mathcal{O}(a^2)$ corrections to Green's functions of local fermion operators that have the form $\bar{\Psi}\Gamma\Psi$. Γ corresponds to the following set of products of the Dirac matrices

$$\Gamma = \mathbb{1}, \gamma^5, \gamma_\mu, \gamma^5\gamma_\mu, \gamma^5\sigma_{\mu\nu}, \quad \sigma_{\mu\nu} = \frac{1}{2}[\gamma_\mu, \gamma_\nu] \quad (27)$$

for the scalar (O^S), pseudoscalar (O^P), vector (O^V), axial (O^A) and tensor (O^T) operator, respectively. We restrict ourselves to forward matrix elements (2-point Green's functions, zero momentum operator insertions). We also considered the tensor operator $O^{T'}$, corresponding to $\Gamma = \sigma_{\mu\nu}$ and checked that the Green's function coincides with that of O^T ; this is a nontrivial check for our calculational procedure.

The only one-particle irreducible Feynman diagram that enters the calculation of the above operators is shown in Fig. 2.

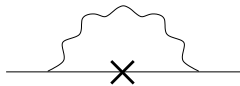


Fig. 2: One-loop diagram contributing to the bilinear operators. A wavy (solid) line represents gluons (fermions). A cross denotes the Dirac matrices $\mathbb{1}$ (scalar), γ^5 (pseudoscalar), γ_μ (vector), $\gamma^5\gamma_\mu$ (axial), $\gamma^5\sigma_{\mu\nu}$ (tensor T) and $\sigma_{\mu\nu}$ (tensor T').

We show our results for the one-loop corrections to the amputated 2-point Green's function of each operator $\bar{\Psi}\Gamma\Psi$, at momentum p

$$\Lambda^\Gamma(p) = \langle \Psi (\bar{\Psi}\Gamma\Psi) \bar{\Psi} \rangle_{(p)}^{amp} \quad (28)$$

Our final results are given as a polynomial of c_{SW} , in a general covariant gauge. Since their dependence on the Symanzik parameters, c_i , cannot be written in a closed form, as in the case of the quark propagator we will tabulate the numerical coefficients for a variety

of choices for c_i , in order to cover a range of values that are used in both perturbative calculations and numerical simulations.

We begin with the $\mathcal{O}(a^2)$ corrected expression for $\Lambda^S(p)$; including the tree-level term, we obtain

$$\begin{aligned}
\Lambda^S(p) = & 1 + \tilde{g}^2 \left[\varepsilon_S^{(0,1)} + 5.79200956(5) \lambda + \varepsilon_S^{(0,2)} c_{\text{SW}} + \varepsilon_S^{(0,3)} c_{\text{SW}}^2 - \ln(a^2 p^2) (3 + \lambda) \right] \\
& + a i \not{p} \tilde{g}^2 \left[\varepsilon_S^{(1,1)} - 3.93575928(1) \lambda + \varepsilon_S^{(1,2)} c_{\text{SW}} + \varepsilon_S^{(1,3)} c_{\text{SW}}^2 + \left(\frac{3}{2} + \lambda + \frac{3}{2} c_{\text{SW}} \right) \ln(a^2 p^2) \right] \\
& + a^2 p^2 \tilde{g}^2 \left[\varepsilon_S^{(2,1)} - 2.27358943(5) \lambda + \varepsilon_S^{(2,2)} c_{\text{SW}} + \varepsilon_S^{(2,3)} c_{\text{SW}}^2 + \left(-\frac{1}{4} + \frac{3}{4} \lambda + \frac{3}{2} c_{\text{SW}} \right) \ln(a^2 p^2) \right] \\
& + a^2 \frac{\sum_{\mu} p_{\mu}^4}{p^2} \tilde{g}^2 \left[\frac{13}{24} + \frac{C_2}{2} - \frac{\lambda}{8} \right] \tag{29}
\end{aligned}$$

The numerical coefficients $\varepsilon_S^{(0,i)}$, $\varepsilon_S^{(1,i)}$ and $\varepsilon_S^{(2,i)}$ with their systematic errors are presented in Tables VIII, IX and X, respectively.

One might attempt to use the $\mathcal{O}(a)$ corrections computed above in order to devise an improved operator, with suppressed finite- a artifacts; it should be noted, however, that improvement by means of local operators, as permitted by Quantum Field Theory, is not sufficient to warrant a complete cancellation of $\mathcal{O}(a^2)$ terms in Green's functions, since the latter contain also terms with non-polynomial momentum dependence, such as $\sum_{\mu} p_{\mu}^4/p^2$. Thus, at best, one can achieve full $\mathcal{O}(a^2)$ improvement only on-shell, or approximate improvement near a given reference momentum scale. Such non-polynomial terms are not present at $\mathcal{O}(a^1)$. This comment applies also to the remaining operators we examine below.

Next, we turn to $\Lambda^P(p)$, where Symanzik dependent coefficients, $\varepsilon_P^{(i,j)}$, are tabulated in Table XI. The pseudoscalar operator is free of $\mathcal{O}(a^1)$ terms; moreover, all contributions linear in c_{SW} vanish

$$\begin{aligned}
\Lambda^P(p) = & \gamma^5 + \gamma^5 \tilde{g}^2 \left[\varepsilon_P^{(0,1)} + 5.79200956(5) \lambda + \varepsilon_P^{(0,2)} c_{\text{SW}}^2 - \ln(a^2 p^2) (3 + \lambda) \right] \\
& + a^2 p^2 \gamma^5 \tilde{g}^2 \left[\varepsilon_P^{(2,1)} - 0.83810121(5) \lambda + \varepsilon_P^{(2,2)} c_{\text{SW}}^2 + \left(-\frac{1}{4} + \frac{\lambda}{4} \right) \ln(a^2 p^2) \right] \\
& + a^2 \frac{\sum_{\mu} p_{\mu}^4}{p^2} \gamma^5 \tilde{g}^2 \left[\frac{13}{24} + \frac{C_2}{2} - \frac{\lambda}{8} \right] \tag{30}
\end{aligned}$$

The $\mathcal{O}(a^2)$ corrected expressions for $\Lambda^V(p)$ and $\Lambda^A(p)$ are more complicated, compared to the scalar and pseudoscalar amputated Green's functions, in the sense that momentum dependence assumes a variety of functional forms; this fact also introduces several coefficients which depend on the Symanzik parameters

$$\begin{aligned}
\Lambda^V(p) = & \gamma_\mu + \frac{\not{p} p_\mu}{p^2} \tilde{g}^2 \left[-2\lambda \right] \\
& + \gamma_\mu \tilde{g}^2 \left[\varepsilon_V^{(0,1)} + 4.79200956(5)\lambda + \varepsilon_V^{(0,2)} c_{\text{SW}} + \varepsilon_V^{(0,3)} c_{\text{SW}}^2 - \lambda \ln(a^2 p^2) \right] \\
& + a i p_\mu \tilde{g}^2 \left[\varepsilon_V^{(1,1)} - 0.93575928(1)\lambda + \varepsilon_V^{(1,2)} c_{\text{SW}} + \varepsilon_V^{(1,3)} c_{\text{SW}}^2 \right. \\
& \quad \left. + (-3 + \lambda + 3 c_{\text{SW}}) \ln(a^2 p^2) \right] \\
& + a^2 \gamma_\mu p_\mu^2 \tilde{g}^2 \left[\varepsilon_V^{(2,1)} + \frac{\lambda}{8} + \varepsilon_V^{(2,2)} c_{\text{SW}} + \varepsilon_V^{(2,3)} c_{\text{SW}}^2 + \left(-\frac{53}{120} + \frac{11}{10} C_2 \right) \ln(a^2 p^2) \right] \\
& + a^2 \gamma_\mu p^2 \tilde{g}^2 \left[\varepsilon_V^{(2,4)} - 0.8110353(1)\lambda + \varepsilon_V^{(2,5)} c_{\text{SW}} + \varepsilon_V^{(2,6)} c_{\text{SW}}^2 \right. \\
& \quad \left. + \left(\frac{11}{240} - \frac{c_1}{2} - \frac{C_2}{60} + \frac{\lambda}{8} - \frac{5}{12} c_{\text{SW}} + \frac{c_{\text{SW}}^2}{4} \right) \ln(a^2 p^2) \right] \\
& + a^2 \not{p} p_\mu \tilde{g}^2 \left[\varepsilon_V^{(2,7)} + 0.2436436(1)\lambda + \varepsilon_V^{(2,8)} c_{\text{SW}} + \varepsilon_V^{(2,9)} c_{\text{SW}}^2 \right. \\
& \quad \left. + \left(-\frac{149}{120} - c_1 - \frac{C_2}{30} + \frac{\lambda}{4} + \frac{c_{\text{SW}}}{6} + \frac{c_{\text{SW}}^2}{2} \right) \ln(a^2 p^2) \right] \\
& + a^2 \gamma_\mu \frac{\sum_\rho p_\rho^4}{p^2} \tilde{g}^2 \left[\frac{3}{80} + \frac{C_2}{10} + \frac{5}{48} \lambda \right] + a^2 \frac{\not{p}^3 p_\mu}{p^2} \tilde{g}^2 \left[-\frac{101}{60} + \frac{11}{15} C_2 + \frac{\lambda}{3} \right] \\
& + a^2 \frac{\not{p} p_\mu^3}{p^2} \tilde{g}^2 \left[-\frac{1}{60} + \frac{2}{5} C_2 + \frac{\lambda}{12} \right] + a^2 \frac{\not{p} p_\mu \sum_\rho p_\rho^4}{(p^2)^2} \tilde{g}^2 \left[-\frac{3}{40} - \frac{C_2}{5} - \frac{5}{24} \lambda \right] \quad (31)
\end{aligned}$$

The numerical values of $\varepsilon_V^{(i,j)}$ for different Symanzik choices are given in Tables XII - XVI.

$$\begin{aligned}
\Lambda^A(p) = & \gamma^5 \gamma_\mu + \frac{\gamma^5 \not{p} p_\mu}{p^2} \tilde{g}^2 \left[-2 \lambda \right] \\
& + \gamma^5 \gamma_\mu \tilde{g}^2 \left[\varepsilon_A^{(0,1)} + 4.79200956(5) \lambda + \varepsilon_A^{(0,2)} c_{\text{SW}} + \varepsilon_A^{(0,3)} c_{\text{SW}}^2 - \lambda \ln(a^2 p^2) \right] \\
& + a i \gamma^5 (\gamma_\mu \not{p} - p_\mu) \tilde{g}^2 \left[\varepsilon_A^{(1,1)} - 2.93575928(1) \lambda \right. \\
& \quad \left. + \varepsilon_A^{(1,2)} c_{\text{SW}} + \varepsilon_A^{(1,3)} c_{\text{SW}}^2 + \lambda \ln(a^2 p^2) \right] \\
& + a^2 \gamma^5 \gamma_\mu p_\mu^2 \tilde{g}^2 \left[\varepsilon_A^{(2,1)} + \frac{\lambda}{8} + \varepsilon_A^{(2,2)} c_{\text{SW}} + \varepsilon_A^{(2,3)} c_{\text{SW}}^2 + \left(-\frac{53}{120} + \frac{11}{10} C_2 \right) \ln(a^2 p^2) \right] \\
& + a^2 \gamma^5 \gamma_\mu p^2 \tilde{g}^2 \left[\varepsilon_A^{(2,4)} - 1.7465235(1) \lambda + \varepsilon_A^{(2,5)} c_{\text{SW}} + \varepsilon_A^{(2,6)} c_{\text{SW}}^2 \right. \\
& \quad \left. + \left(-\frac{109}{240} - \frac{c_1}{2} - \frac{C_2}{60} + \frac{5}{8} \lambda + \frac{7}{12} c_{\text{SW}} - \frac{c_{\text{SW}}^2}{4} \right) \ln(a^2 p^2) \right] \\
& + a^2 \gamma^5 \not{p} p_\mu \tilde{g}^2 \left[\varepsilon_A^{(2,7)} + 1.1146200(1) \lambda + \varepsilon_A^{(2,8)} c_{\text{SW}} + \varepsilon_A^{(2,9)} c_{\text{SW}}^2 \right. \\
& \quad \left. + \left(\frac{91}{120} - c_1 - \frac{C_2}{30} - \frac{3}{4} \lambda - \frac{5}{6} c_{\text{SW}} - \frac{c_{\text{SW}}^2}{2} \right) \ln(a^2 p^2) \right] \\
& + a^2 \gamma^5 \gamma_\mu \frac{\sum_\rho p_\rho^4}{p^2} \tilde{g}^2 \left[\frac{3}{80} + \frac{C_2}{10} + \frac{5}{48} \lambda \right] + a^2 \gamma^5 \frac{\not{p}^3 p_\mu}{p^2} \tilde{g}^2 \left[-\frac{101}{60} + \frac{11}{15} C_2 + \frac{\lambda}{3} \right] \\
& + a^2 \gamma^5 \frac{\not{p} p_\mu^3}{p^2} \tilde{g}^2 \left[-\frac{1}{60} + \frac{2}{5} C_2 + \frac{\lambda}{12} \right] + a^2 \gamma^5 \frac{\not{p} p_\mu \sum_\rho p_\rho^4}{(p^2)^2} \tilde{g}^2 \left[-\frac{3}{40} - \frac{C_2}{5} - \frac{5}{24} \lambda \right] \quad (32)
\end{aligned}$$

Eq. (31) and Eq. (32) have many similar terms, among them the coefficients

$$\varepsilon_A^{(0,2)} = -\varepsilon_V^{(0,2)}, \quad \varepsilon_A^{(0,3)} = -\varepsilon_V^{(0,3)} \quad (33)$$

The rest of the coefficients $\varepsilon_A^{(i,j)}$ appear in Tables XVII - XX.

The remaining Green's functions that we computed are those corresponding to the tensor bilinears ($T = \gamma^5 \sigma_{\mu\nu}$, $T' = \sigma_{\mu\nu}$), which are the most complicated of all the operators that we studied. Clearly, the Green's functions $\Lambda^T(p)$ and $\Lambda^{T'}(p)$, corresponding to T and T' , coincide numerically, even though this fact is not immediately apparent from their algebraic forms. In fact, we computed both $\Lambda^T(p)$ and $\Lambda^{T'}(p)$ in two distinct calculations; their numerical coincidence constitutes a rather nontrivial check of our results. For the reader's

convenience, we present below both tensor Green's functions.

$$\begin{aligned}
\Lambda^T(p) = & \gamma^5 \sigma_{\mu\nu} + \gamma^5 \sigma_{\mu\nu} \tilde{g}^2 \left[\varepsilon_T^{(0,1)} + 3.79200956(5) \lambda + \varepsilon_T^{(0,2)} c_{\text{SW}} + \varepsilon_T^{(0,3)} c_{\text{SW}}^2 + (1 - \lambda) \ln(a^2 p^2) \right] \\
& + a i \gamma^5 \frac{(\gamma_\nu p_\mu - \gamma_\mu p_\nu)}{2} \tilde{g}^2 \left[\varepsilon_T^{(1,1)} + 3.87151852(5) \lambda + \varepsilon_T^{(1,2)} c_{\text{SW}} + \varepsilon_T^{(1,3)} c_{\text{SW}}^2 \right. \\
& \quad \left. + (3 - 2\lambda - c_{\text{SW}}) \ln(a^2 p^2) \right] \\
& + a^2 \gamma^5 \frac{(\gamma_\mu \gamma_\nu p_\mu^2 - \gamma_\nu \gamma_\mu p_\nu^2)}{2} \tilde{g}^2 \left[\varepsilon_T^{(2,1)} + \frac{\lambda}{4} + \varepsilon_T^{(2,2)} c_{\text{SW}} + \varepsilon_T^{(2,3)} c_{\text{SW}}^2 \right] \\
& + a^2 \gamma^5 \frac{(\gamma_\nu \not{p} p_\mu - \gamma_\mu \not{p} p_\nu)}{2} \tilde{g}^2 \left[\varepsilon_T^{(2,4)} + 0.62097643(2) \lambda + \varepsilon_T^{(2,5)} c_{\text{SW}} + \varepsilon_T^{(2,6)} c_{\text{SW}}^2 \right. \\
& \quad \left. + (2 - \lambda - c_{\text{SW}}) \ln(a^2 p^2) \right] \\
& + a^2 \gamma^5 \sigma_{\mu\nu} p^2 \tilde{g}^2 \left[\varepsilon_T^{(2,7)} - 0.7839694(1) \lambda + \varepsilon_T^{(2,8)} c_{\text{SW}} + \varepsilon_T^{(2,9)} c_{\text{SW}}^2 \right. \\
& \quad \left. + \left(\frac{1}{12} - c_1 + \frac{C_2}{3} - \frac{c_{\text{SW}}}{2} \right) \ln(a^2 p^2) \right] \\
& + a^2 \gamma^5 \frac{(\gamma_\nu \not{p} p_\mu^3 - \gamma_\mu \not{p} p_\nu^3)}{2 p^2} \tilde{g}^2 \left[-\frac{1}{2} + C_2 + \frac{\lambda}{2} \right] + a^2 \gamma^5 \frac{(p_\mu^3 p_\nu - p_\nu^3 p_\mu)}{2 p^2} \tilde{g}^2 \left[\frac{17}{3} + \frac{2}{3} C_2 \right] \\
& + a^2 \gamma^5 \frac{(\gamma_\nu \not{p}^3 p_\mu - \gamma_\mu \not{p}^3 p_\nu)}{2 p^2} \tilde{g}^2 \left[\frac{17}{6} + \frac{C_2}{3} \right] + a^2 \gamma^5 \sigma_{\mu\nu} \frac{\sum_\rho p_\rho^4}{p^2} \tilde{g}^2 \left[-\frac{1}{3} + \frac{C_2}{2} + \frac{\lambda}{3} \right] \\
& + a^2 \gamma^5 \frac{(\gamma_\mu \not{p} p_\mu^2 p_\nu - \gamma_\nu \not{p} p_\mu p_\nu^2)}{2 p^2} \tilde{g}^2 \left[-\frac{7}{3} - \frac{4}{3} C_2 - \frac{\lambda}{2} \right] \tag{34}
\end{aligned}$$

The coefficients $\varepsilon_T^{(i,j)}$ are tabulated in Tables XXI - XXV.

$$\begin{aligned}
\Lambda^{T'}(p) = & \sigma_{\mu\nu} + \sigma_{\mu\nu} \tilde{g}^2 \left[\varepsilon_{T'}^{(0,1)} + 3.79200956(5) \lambda + \varepsilon_{T'}^{(0,2)} c_{\text{SW}} + \varepsilon_{T'}^{(0,3)} c_{\text{SW}}^2 + (1 - \lambda) \ln(a^2 p^2) \right] \\
& + a i \frac{(\gamma_\nu p_\mu - \gamma_\mu p_\nu) + \sigma_{\mu\nu} \not{p}}{2} \tilde{g}^2 \left[\varepsilon_{T'}^{(1,1)} - 3.87151852(5) \lambda + \varepsilon_{T'}^{(1,2)} c_{\text{SW}} + \varepsilon_{T'}^{(1,3)} c_{\text{SW}}^2 \right. \\
& \quad \left. + (-3 + 2\lambda + c_{\text{SW}}) \ln(a^2 p^2) \right] \\
& + a^2 \frac{(\gamma_\mu \gamma_\nu p_\mu^2 - \gamma_\nu \gamma_\mu p_\nu^2)}{2} \tilde{g}^2 \left[\varepsilon_{T'}^{(2,1)} + \frac{\lambda}{4} + \varepsilon_{T'}^{(2,2)} c_{\text{SW}} + \varepsilon_{T'}^{(2,3)} c_{\text{SW}}^2 \right] \\
& + a^2 \frac{(\gamma_\nu \not{p} p_\mu - \gamma_\mu \not{p} p_\nu)}{2} \tilde{g}^2 \left[\varepsilon_{T'}^{(2,4)} - 1.12097643(1) \lambda + \varepsilon_{T'}^{(2,5)} c_{\text{SW}} + \varepsilon_{T'}^{(2,6)} c_{\text{SW}}^2 \right. \\
& \quad \left. + (-2 + \lambda + c_{\text{SW}}) \ln(a^2 p^2) \right] \\
& + a^2 \sigma_{\mu\nu} p^2 \tilde{g}^2 \left[\varepsilon_{T'}^{(2,7)} - 1.2194576(1) \lambda + \varepsilon_{T'}^{(2,8)} c_{\text{SW}} + \varepsilon_{T'}^{(2,9)} c_{\text{SW}}^2 \right. \\
& \quad \left. + \left(-\frac{11}{12} - c_1 + \frac{C_2}{3} + \frac{\lambda}{2} \right) \ln(a^2 p^2) \right] \\
& + a^2 \frac{(\gamma_\nu \not{p} p_\mu^3 - \gamma_\mu \not{p} p_\nu^3)}{2 p^2} \tilde{g}^2 \left[-\frac{1}{2} + C_2 + \frac{\lambda}{2} \right] + a^2 \frac{(p_\mu^3 p_\nu - p_\nu^3 p_\mu)}{2 p^2} \tilde{g}^2 \left[\frac{17}{3} + \frac{2}{3} C_2 \right] \\
& + a^2 \frac{(\gamma_\nu \not{p}^3 p_\mu - \gamma_\mu \not{p}^3 p_\nu)}{2 p^2} \tilde{g}^2 \left[\frac{17}{6} + \frac{C_2}{3} \right] + a^2 \sigma_{\mu\nu} \frac{\sum_\rho p_\rho^4}{p^2} \tilde{g}^2 \left[-\frac{1}{3} + \frac{C_2}{2} + \frac{\lambda}{3} \right] \\
& + a^2 \frac{(\gamma_\mu \not{p} p_\mu^2 p_\nu - \gamma_\nu \not{p} p_\mu p_\nu^2)}{2 p^2} \tilde{g}^2 \left[-\frac{7}{3} - \frac{4}{3} C_2 - \frac{\lambda}{2} \right] \tag{35}
\end{aligned}$$

Several coefficients $\varepsilon_{T'}$ can be written in terms of ε_T (Eqs. (36) - (38)), while the rest are given in Tables XXVI - XXVII

$$\varepsilon_{T'}^{(0,1)} = \varepsilon_T^{(0,1)}, \quad \varepsilon_{T'}^{(0,2)} = \varepsilon_T^{(0,2)}, \quad \varepsilon_{T'}^{(0,3)} = \varepsilon_T^{(0,3)}, \tag{36}$$

$$\varepsilon_{T'}^{(1,1)} = -\varepsilon_T^{(1,1)}, \quad \varepsilon_{T'}^{(1,2)} = -\varepsilon_T^{(1,2)}, \quad \varepsilon_{T'}^{(1,3)} = -\varepsilon_T^{(1,3)}, \tag{37}$$

$$\varepsilon_{T'}^{(2,2)} = -\varepsilon_T^{(2,2)}, \quad \varepsilon_{T'}^{(2,3)} = -\varepsilon_T^{(2,3)}, \quad \varepsilon_{T'}^{(2,5)} = -\varepsilon_T^{(2,5)}, \quad \varepsilon_{T'}^{(2,6)} = -\varepsilon_T^{(2,6)} \tag{38}$$

VI. DISCUSSION AND CONCLUSIONS

In this paper we have calculated the fermion propagator $S(p)$ and the Green's functions $\Lambda^\Gamma(p)$ for the fermion bilinear operators $\bar{\Psi}\Gamma\Psi$, where Γ stands for any product of Dirac

gamma matrices. Our calculations were performed to one loop in lattice perturbation theory, using the Wilson/clover fermion action. For gluons we employed a family of Symanzik improved actions, parameterized by 3 independent ‘‘Symanzik’’ coefficients; explicit results are presented for some of the most commonly used actions in this family: Wilson, Tree-level Symanzik, Tadpole improved Lüscher-Weisz, Iwasaki and DBW2.

Our calculations extend, to a rather large family of fermion/gluon actions, results which were previously known to $\mathcal{O}(a^0)$ and $\mathcal{O}(a^1)$ (modulo $\ln a$). However, the truly novel feature in our calculations is that they were performed to second order in the lattice spacing a ($\mathcal{O}(a^2, a^2 \ln a)$). This fact introduces a number of complications, which are not present in lower order results. In a nutshell, the reason for these complications is as follows: The extraction of a further power of a from a Feynman diagram strengthens, by one unit, the superficial degree of infrared (IR) divergence of the corresponding integrand over loop momenta. Thus, a priori, in a $\mathcal{O}(a^1)$ calculation, loop integrals would be IR convergent only in $D > 5$ dimensions; however, as can be easily deduced by inspection, the most divergent parts of the integrands are odd functions of the loop momenta, and will thus vanish upon integration. What is left behind is a less divergent integrand which is IR convergent in $D > 4$, just as in the case of $\mathcal{O}(a^0)$ calculations, and can thus be treated by standard methods, such as those of Ref. [25]. For $\mathcal{O}(a^2)$ calculations, on the other hand, integrands are IR convergent only at $D > 6$, and their most divergent parts no longer vanish upon integration; a naive application of the procedure of Ref. [25] will fail to produce all $\mathcal{O}(a^2)$ contributions. The procedure which we propose in this work for handling the above difficulty is in fact applicable to any order in a . In brief, it recasts the integrands as a sum of two parts: The first part can be *exactly* evaluated as a function of a , while the second part is naively Taylor expandible, as a polynomial to the desired order in a .

Since the propagator and Green’s functions are meant to be used in mass independent renormalization schemes, our results have been obtained at vanishing fermionic masses; the case of massive fermions (including non-degenerate flavors and twisted mass terms) will appear in a forthcoming publication. Nevertheless, even at vanishing masses, our final expressions are quite lengthy, since they exhibit a rather nontrivial dependence on the external momentum (p), and they are explicit functions of the number of colors (N), gauge parameter (λ), lattice spacing (a), clover coefficient (c_{SW}) and coupling constant (g); furthermore,

most numerical coefficients in these expressions depend on the Symanzik parameters of the gluon action, and we have tabulated them for the actions we have selected. For convenience, we accompany this paper with an electronic document, in the form of a Mathematica input file, allowing the reader to recover immediately numerical values for any choice of input parameters.

One possible use of our results is in constructing improved versions of the operators O^Γ , with reduced lattice artifacts. In doing so, however, one must bear in mind that, unlike the $\mathcal{O}(a^1)$ case, corrections to $\mathcal{O}(a^2)$ include expressions which are non-polynomial in the external momentum and, therefore, cannot be eliminated by introducing admixtures of local operators. Full improvement can be achieved at best for on-shell matrix elements only.

Starting from $S(p)$ and $\Lambda^\Gamma(p)$, it is straightforward to write down the renormalization functions Z_q (for the quark field) and Z_Γ (for the operators O^Γ) in any renormalization scheme. Z_q and Z_Γ , as obtained from $S(p)$ and $\Lambda^\Gamma(p)$, differ from the corresponding expressions evaluated at $\mathcal{O}(a^0)$, by lattice artefact, which are functions of $(a\mu)$ (μ : renormalization scale), and vanish as $a \rightarrow 0$. At the nonzero values of a employed in numerical simulations, these factors are quite important. Ideally, one would prefer a nonperturbative determination of renormalization functions; while this is often possible, several sources of error must be dealt with. A very effective way to proceed is through a combination of perturbative and nonperturbative results. This procedure is carried out and explained in detail in a follow-up work [22]. Briefly stated, nonperturbative data are “corrected” by the perturbative expressions for Green’s functions, and then extrapolated towards small a . As a first illustration of this mixed determination, we show in Fig. 3 nonperturbative data for Z_q and Z_V , determined with the RI-MOM method of Ref. [23], before and after the perturbative corrections. The results are obtained by using the Symanzik tree-level improved gluon action at $\beta = 3.9$ and the $N_f = 2$ twisted mass quark action at maximal twist, with gauge field configurations and quark propagators generated by the ETM Collaboration³. While up to discretization effects Z_V is a scale independent quantity, the (continuum) RG dependence of Z_q on the renormalization scale has been removed from the results shown in Fig. 3 by evolving the renormalization constant to a fixed reference scale $\mu_0 = 1/a$ (~ 2 GeV), using for the

³ We thank the members of the ETM Collaboration for having provided us with the data of Fig. 3 before publication.

anomalous dimension the 4-loop perturbative expression computed in Ref. [27]. Thus, the residual dependence of both $Z_q(\mu_0 = 1/a)$ and Z_V on $a^2\tilde{p}^2$ observed in Fig. 3 can be safely interpreted, at large momenta, as a pure discretization effect. As illustrated in Fig. 3, the corrected data are virtually flat, allowing for a safer small- a extrapolation.

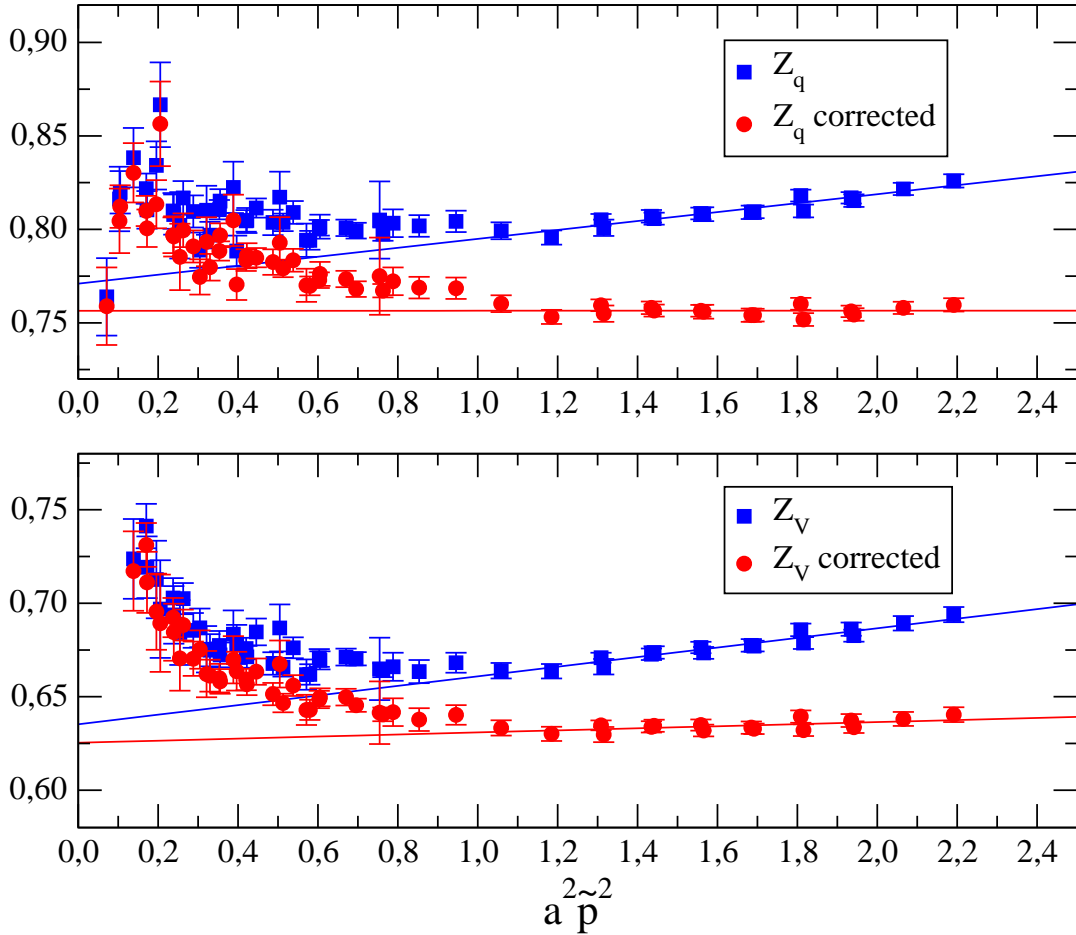


Fig. 3: Non-perturbative data for $Z_q(\mu_0 = 1/a)$ and Z_V , before and after perturbative corrections. Straight lines are extrapolations to small a . ($a^2\tilde{p}^2 \equiv \sum_{\mu} \sin^2(ap_{\mu})$)

The techniques employed in this work are readily applicable to the study of perturbative

corrections of other Greens's functions, to any desired order in a . Examples are matrix elements of 4-fermion operators appearing in effective weak Hamiltonians, and higher dimension twist-2 fermion bilinears involved in generalized parton distributions. We will be addressing these issues in forthcoming publications.

APPENDIX A: A BASIS OF DIVERGENT INTEGRALS

The most difficult part of this calculation that requires careful attention is the extraction of the dependence on the external momentum p and the lattice spacing a from the divergent terms. The singularities are isolated using the procedure explained in section II, and here we present the list of primitively divergent integrals that appeared in our algebraic expressions.

In the following integrals we define

$$\begin{aligned}\hat{k}_\mu &= 2 \sin\left(\frac{k_\mu}{2}\right) \\ \hat{k}^2 &= 4 \sum_\mu \sin^2\left(\frac{k_\mu}{2}\right) \\ \overset{\circ}{k}_\mu &= \sin(k_\mu)\end{aligned}$$

In addition, $(\)_S$ means sum over inequivalent permutations. No summation over the indices μ, ν, ρ, σ is implied, unless otherwise stated.

$$\begin{aligned}\bullet \int_{-\pi}^{\pi} \frac{d^4 k}{(2\pi)^4} \frac{1}{\hat{k}^2 \widehat{k + ap}^2} &= 0.036678329075 - \frac{\ln(a^2 p^2)}{16\pi^2} \\ &+ 0.0000752406(3) a^2 p^2 + a^2 \frac{\sum_\mu p_\mu^4}{384\pi^2 p^2} + \mathcal{O}(a^4 p^4)\end{aligned}\quad (\text{A1})$$

$$\begin{aligned}\bullet \int_{-\pi}^{\pi} \frac{d^4 k}{(2\pi)^4} \frac{\overset{\circ}{k}_\mu}{\hat{k}^2 \widehat{k + ap}^2} &= a p_\mu \left[-0.008655827648 + \frac{\ln(a^2 p^2)}{32\pi^2} \right. \\ &- 0.0005107825(2) a^2 p^2 + 0.001171329715 a^2 p_\mu^2 \\ &\left. - a^2 \frac{\sum_\mu p_\mu^4}{768\pi^2 p^2} + a^2 \frac{\ln(a^2 p^2)}{384\pi^2} \left(\frac{p^2}{2} - p_\mu^2 \right) \right] \\ &+ \mathcal{O}(a^5 p^5)\end{aligned}\quad (\text{A2})$$

$$\begin{aligned}
\bullet \int_{-\pi}^{\pi} \frac{d^4 k}{(2\pi)^4} \frac{\overset{\circ}{k}_\mu \overset{\circ}{k}_\nu}{(\hat{k}^2)^2 \widehat{k + a p}^2} &= \delta_{\mu\nu} \left[0.004327913824 - \frac{\ln(a^2 p^2)}{64\pi^2} \right. \\
&\quad + 0.00025539124(8) a^2 p^2 - 0.000135654113 a^2 p_\mu^2 \\
&\quad \left. + a^2 \frac{\sum_\mu p_\mu^4}{1536\pi^2 p^2} + a^2 \frac{\ln(a^2 p^2)}{768\pi^2} \left(p_\mu^2 - \frac{p^2}{2} \right) \right] \\
&\quad + a^2 p_\mu p_\nu \left[\frac{1}{32\pi^2 a^2 p^2} - 0.0003788538(2) + \frac{\sum_\mu p_\mu^4}{768\pi^2 (p^2)^2} \right. \\
&\quad \left. - \frac{(p_\mu^2 + p_\nu^2)}{384\pi^2 p^2} + \frac{\ln(a^2 p^2)}{768\pi^2} \right] + \mathcal{O}(a^4 p^4) \tag{A3}
\end{aligned}$$

$$\begin{aligned}
\bullet \int_{-\pi}^{\pi} \frac{d^4 k}{(2\pi)^4} \frac{\overset{\circ}{k}_\mu \overset{\circ}{k}_\nu}{\hat{k}^2 \widehat{k + a p}^2} &= \delta_{\mu\nu} \left[0.014966695116 - 0.001256484446 a^2 p^2 \right. \\
&\quad \left. - 0.001027789631 a^2 p_\mu^2 + \frac{a^2 p^2 \ln(a^2 p^2)}{192\pi^2} \right] \\
&\quad + a^2 p_\mu p_\nu \left[0.003970508789 - \frac{\ln(a^2 p^2)}{48\pi^2} \right] + \mathcal{O}(a^4 p^4) \tag{A4}
\end{aligned}$$

$$\begin{aligned}
\bullet \int_{-\pi}^{\pi} \frac{d^4 k}{(2\pi)^4} \frac{(\overset{\circ}{k}_\mu)^3}{\hat{k}^2 \widehat{k + a p}^2} &= a p_\mu \left[-0.006184131744 + 0.001102333439 a^2 p^2 \right. \\
&\quad \left. - 0.000174224479 a^2 p_\mu^2 + a^2 \frac{\ln(a^2 p^2)}{64\pi^2} \left(p_\mu^2 - \frac{p^2}{2} \right) \right] \\
&\quad + \mathcal{O}(a^5 p^5) \tag{A5}
\end{aligned}$$

$$\begin{aligned}
\bullet \int_{-\pi}^{\pi} \frac{d^4 k}{(2\pi)^4} \frac{\overset{\circ}{k}_\mu \overset{\circ}{k}_\nu \overset{\circ}{k}_\rho}{(\hat{k}^2)^2 \widehat{k + a p}^2} &= (\delta_{\nu\rho} a p_\mu)_S \left[-0.000728769948 + \frac{\ln(a^2 p^2)}{192\pi^2} \right] \\
&\quad + 0.001027789631 \delta_{\mu\nu\rho} a p_\mu - a \frac{p_\mu p_\nu p_\rho}{48\pi^2 p^2} + \mathcal{O}(a^3 p^3) \tag{A6}
\end{aligned}$$

$$\begin{aligned}
\bullet \int_{-\pi}^{\pi} \frac{d^4 k}{(2\pi)^4} \frac{\sum_{\mu} \hat{k}_{\mu}^4}{16(\hat{k}^2)^2 \widehat{k+a p}^2} &= 0.004050096698 - 0.000107954163 a^2 p^2 + a^2 \frac{\sum_{\mu} p_{\mu}^4}{1024\pi^2 p^2} \\
&+ \mathcal{O}(a^4 p^4)
\end{aligned} \tag{A7}$$

$$\begin{aligned}
\bullet \int_{-\pi}^{\pi} \frac{d^4 k}{(2\pi)^4} \frac{\overset{\circ}{k}_{\mu} \overset{\circ}{k}_{\nu} \overset{\circ}{k}_{\rho} \overset{\circ}{k}_{\sigma}}{(\hat{k}^2)^2 \widehat{k+a p}^2} &= 0.001589337971 (\delta_{\mu\nu} \delta_{\rho\sigma})_S - 0.001675948042 \delta_{\mu\nu\rho\sigma} \\
&- 0.000372782983 (\delta_{\mu\nu\rho} a^2 p_{\mu} p_{\sigma})_S - 0.000062130497 (\delta_{\mu\nu} \delta_{\rho\sigma} a^2 p_{\mu}^2)_S \\
&+ \delta_{\mu\nu\rho\sigma} (0.000186391491 a^2 p^2 + 0.000410290033 a^2 p_{\mu}^2) \\
&+ (\delta_{\mu\nu} a^2 p_{\rho} p_{\sigma})_S \left(0.000227848225 - \frac{\ln(a^2 p^2)}{384\pi^2} \right) \\
&+ (\delta_{\mu\nu} \delta_{\rho\sigma})_S a^2 p^2 \left(-0.000245852737 + \frac{\ln(a^2 p^2)}{768\pi^2} \right) \\
&+ a^2 \frac{p_{\mu} p_{\nu} p_{\rho} p_{\sigma}}{64\pi^2 p^2} + \mathcal{O}(a^4 p^4)
\end{aligned} \tag{A8}$$

$$\begin{aligned}
\bullet \int_{-\pi}^{\pi} \frac{d^4 k}{(2\pi)^4} \frac{\overset{\circ}{k}_{\nu} \sum_{\mu} \hat{k}_{\mu}^4}{16(\hat{k}^2)^2 \widehat{k+a p}^2} &= a p_{\nu} \left[-0.000800034900 + 0.000069705553 a^2 p^2 \right. \\
&+ 0.000107082394 a^2 p_{\nu}^2 - a^2 \frac{\sum_{\rho} p_{\rho}^4}{1280\pi^2 p^2} \\
&\left. - a^2 \frac{\ln(a^2 p^2)}{2560\pi^2} \left(\frac{p^2}{2} - p_{\nu}^2 \right) \right] + \mathcal{O}(a^5 p^5)
\end{aligned} \tag{A9}$$

$$\begin{aligned}
\bullet \int_{-\pi}^{\pi} \frac{d^4 k}{(2\pi)^4} \frac{\overset{\circ}{k}_{\nu} \overset{\circ}{k}_{\rho} \sum_{\mu} \widehat{k_{\mu} + a p_{\mu}}^4}{16(\hat{k}^2)^2 (\widehat{k+a p}^2)^2} &= \delta_{\nu\rho} \left[0.000400017450 - 0.000034852777 a^2 p^2 + a^2 \frac{\sum_{\mu} p_{\mu}^4}{2560\pi^2 p^2} \right. \\
&+ 0.000105349447 a^2 p_{\nu}^2 + a^2 \frac{\ln(a^2 p^2)}{5120\pi^2} \left(\frac{p^2}{2} - 3p_{\nu}^2 \right) \left. \right] \\
&+ a^2 p_{\nu} p_{\rho} \left[0.000006643045 - \frac{p_{\nu}^2 + p_{\rho}^2}{2560\pi^2 p^2} + \frac{\sum_{\mu} p_{\mu}^4}{5120\pi^2 (p^2)^2} \right. \\
&\left. + \frac{\ln(a^2 p^2)}{5120\pi^2} \right] + \mathcal{O}(a^4 p^4)
\end{aligned} \tag{A10}$$

Acknowledgments: This work is supported in part by the Research Promotion Foundation of Cyprus (Proposal Nr: ENISX/0505/45, TEXN/0308/17).

- [1] K. Symanzik, Nucl. Phys. **B226** (1983) 187; Nucl. Phys. **B226** (1983) 205
- [2] R. Frezzotti, P. Grassi, S. Sint, P. Weisz, JHEP **08** (2001) 058 [hep-lat/0101001].
- [3] R. Frezzotti, G. Rossi, JHEP **08** (2004) 007 [hep-lat/0306014].
- [4] G. Martinelli and Y. Zhang, Phys. Lett. **123B** (1983) 433.
- [5] S. Aoki, K. Nagai, Y. Taniguchi and A. Ukawa, Phys. Rev. **D58** (1998) 074505 [hep-lat/9802034].
- [6] S. Capitani et al., Nucl. Phys. **B593** (2001) 183 [hep-lat/0007004].
- [7] C. Alexandrou, E. Follana, H. Panagopoulos and E. Vicari, Nucl.Phys. **B580** (2000) 394 [hep-lat/0002010].
- [8] S. Capitani and L. Giusti, Phys. Rev. **D62** (2000) 114506 [hep-lat/0007011].
- [9] R. Horsley et al., Nucl. Phys. **B693** (2004) 3; Erratum-ibid. **B713** (2005) 601 [hep-lat/0404007].
- [10] M. Ioannou and H. Panagopoulos, Phys. Rev. **D73** (2006) 054507 [hep-lat/0601020].
- [11] S. Aoki, K. Nagai, Y. Taniguchi, A. Ukawa, Phys. Rev. **D58** (1998) 074505 [hep-lat/9802034].
- [12] A. Skouroupathis, H. Panagopoulos, Phys. Rev. **D76** (2007) 094514 [arXiv:0707.2906].
- [13] A. Skouroupathis, H. Panagopoulos, Two-loop renormalization of vector, axial-vector and tensor fermion bilinears on the lattice, Phys. Rev. **D79** (2009) 094508 [arXiv:0811.4264].
- [14] F. Di Renzo, V. Miccio, L. Scorzato and C. Torrero, PoS LAT2006 (2006) 156 [hep-lat/0609077].
- [15] F. Di Renzo, V. Miccio, L. Scorzato and C. Torrero, Eur. Phys. J. **C51** (2007) 645 [hep-lat/0611013].
- [16] F. Di Renzo, L. Scorzato and C. Torrero, PoS LAT2007 (2007) 240 [arXiv:0710.0552].
- [17] Y. Iwasaki, Univ. of Tsukuba Report UTHEP-118 (1983).
- [18] T. Takaishi, Phys. Rev. **D54** (1996) 1050.
- [19] M. Lüscher and P. Weisz, Commun. Math. Phys. **97** (1985) 59; Erratum-ibid. **98** (1985) 433.

- [20] M. G. Alford, W. Dimm, G. P. Lepage, G. Hockney and P. B. Mackenzie, Phys. Lett. B 361 (1995) 87 [hep-lat/9507010].
- [21] K. Osterwalder and E. Seiler, Ann. Phys. (NY) 110 (1978) 440.
- [22] P. Dimopoulos et al., PoS LAT2007 (2007) 241 [arXiv:0710.0975]; ETM Collaboration, in preparation.
- [23] G. Martinelli, C. Pittori, C. T. Sachrajda, M. Testa and A. Vladikas, Nucl. Phys. B **445** (1995) 81 [hep-lat/9411010].
- [24] H. Panagopoulos, E. Vicari, Nucl. Phys. **B332** (1990) 261.
- [25] H. Kawai, R. Nakayama, K. Seo, Nucl. Phys. **B189** (1981) 40.
- [26] K.G. Chetyrkin and F.V. Tkachov, Nucl. Phys. **B192** (1981) 159.
- [27] K. G. Chetyrkin and A. Retey, Nucl. Phys. B **583** (2000) 3 [arXiv:hep-ph/9910332].

Action	c_0	c_1	c_3
Plaquette	1.0	0	0
Symanzik	1.6666667	-0.0833333	0
TILW, $\beta_{c_0} = 8.60$	2.3168064	-0.151791	-0.0128098
TILW, $\beta_{c_0} = 8.45$	2.3460240	-0.154846	-0.0134070
TILW, $\beta_{c_0} = 8.30$	2.3869776	-0.159128	-0.0142442
TILW, $\beta_{c_0} = 8.20$	2.4127840	-0.161827	-0.0147710
TILW, $\beta_{c_0} = 8.10$	2.4465400	-0.165353	-0.0154645
TILW, $\beta_{c_0} = 8.00$	2.4891712	-0.169805	-0.0163414
Iwasaki	3.648	-0.331	0
DBW2	12.2688	-1.4086	0

TABLE I: Input parameters c_0 , c_1 , c_3 .

Action	$\varepsilon^{(0,1)}$	$\varepsilon^{(0,2)}$	$\varepsilon^{(0,3)}$
Plaquette	16.6444139(2)	-2.24886853(7)	-1.39726711(7)
Symanzik	13.02327272(7)	-2.01542504(4)	-1.24220271(2)
TILW (8.45)	10.82273528(9)	-1.84838009(3)	-1.13513794(1)
TILW (8.00)	10.45668970(6)	-1.81821854(5)	-1.11582732(3)
Iwasaki	8.1165665(2)	-1.60101088(7)	-0.97320689(3)
DBW2	2.9154231(2)	-0.96082198(5)	-0.56869876(4)

TABLE II: The coefficients $\varepsilon^{(0,i)}$ (Eq. (24)) for different actions.

Action	$\varepsilon^{(1,1)}$	$\varepsilon^{(1,2)}$	$\varepsilon^{(1,3)}$
Plaquette	12.8269254(2)	-5.20234231(6)	-0.08172763(4)
Symanzik	10.69642966(8)	-4.7529781(1)	-0.075931174(1)
TILW (8.45)	9.2865455(1)	-4.4186677(2)	-0.07160078(1)
TILW (8.00)	9.0430829(2)	-4.35681290(3)	-0.070688697(3)
Iwasaki	7.40724287(1)	-3.88883584(9)	-0.061025650(8)
DBW2	3.0835163(2)	-2.2646221(1)	-0.03366740(1)

TABLE III: The coefficients $\varepsilon^{(1,i)}$ (Eq. (24)) for different actions.

Action	$\varepsilon^{(2,1)}$	$\varepsilon^{(2,2)}$	$\varepsilon^{(2,3)}$
Plaquette	-4.74536466(2)	0.02028705(5)	0.10348577(3)
Symanzik	-4.2478783(2)	0.05136635(6)	0.07865292(7)
TILW (8.45)	-3.8139475(2)	0.05751390(9)	0.06651692(3)
TILW (8.00)	-3.7342556(1)	0.05830392(9)	0.06444077(4)
Iwasaki	-3.2018047(1)	0.08249970(7)	0.04192446(4)
DBW2	-0.8678072(2)	0.1024452(2)	-0.00343999(2)

TABLE IV: The coefficients $\varepsilon^{(2,1)} - \varepsilon^{(2,3)}$ (Eq. (24)) for different actions.

Action	$\varepsilon^{(2,4)}$	$\varepsilon^{(2,5)}$	$\varepsilon^{(2,6)}$
Plaquette	-1.5048070(1)	0.70358496(5)	0.534320852(7)
Symanzik	-1.14716212(5)	0.65343092(3)	0.49783419(2)
TILW (8.45)	-0.92583451(6)	0.62061757(5)	0.467966296(9)
TILW (8.00)	-0.8875297(1)	0.61441084(7)	0.462237852(9)
Iwasaki	-0.6202244(1)	0.55587473(6)	0.41846440(4)
DBW2	-0.3202477(5)	0.34886590(2)	0.23968038(4)

TABLE V: The coefficients $\varepsilon^{(2,4)} - \varepsilon^{(2,6)}$ (Eq. (24)) for different actions.

Action	$\tilde{\varepsilon}_1^{(0,1)}$	$\tilde{\varepsilon}_1^{(1,1)}$	$\tilde{\varepsilon}_1^{(2,1)}$
Plaquette	9.174787621(1)	4.5873938103(5)	-1.5291312701(2)
Symanzik	7.071174701(5)	3.535587351(2)	-1.1785291169(8)
TILW (8.45)	5.86097856(2)	2.930489282(8)	-0.976829761(3)
TILW (8.00)	5.663791993(4)	2.831895997(2)	-0.9439653322(7)
Iwasaki	4.423664730(5)	2.211832365(2)	-0.7372774550(8)
DBW2	1.86908767(4)	0.93454384(2)	-0.311514612(6)

TABLE VI: The coefficients $\tilde{\varepsilon}_1^{(0,i)}$ (Eq. (25)) for different actions.

Action	$\tilde{\varepsilon}_2^{(0,1)}$	$\tilde{\varepsilon}_2^{(1,1)}$	$\tilde{\varepsilon}_2^{(2,1)}$
Plaquette	7.4696262(2)	8.2395316(2)	-3.21623339(2)
Symanzik	5.95209802(7)	7.16084231(8)	-3.0693492(2)
TILW (8.45)	4.96175672(9)	6.3560562(1)	-2.8371177(2)
TILW (8.00)	4.79289770(6)	6.2111869(2)	-2.7902902(1)
Iwasaki	3.6929018(2)	5.19541051(1)	-2.4645273(1)
DBW2	1.0463355(2)	2.1489724(2)	-0.5562925(2)

TABLE VII: The coefficients $\tilde{\varepsilon}_2^{(0,i)}$ (Eq. (26)) for different actions.

Action	$\varepsilon_S^{(0,1)}$	$\varepsilon_S^{(0,2)}$	$\varepsilon_S^{(0,3)}$
Plaquette	0.30799634(6)	9.9867847(2)	0.01688643(6)
Symanzik	0.58345905(5)	8.8507071(1)	-0.12521126(5)
TILW (8.45)	0.7049818(1)	8.0538938(2)	-0.20881716(3)
TILW (8.00)	0.7195566(1)	7.9115477(2)	-0.22196498(3)
Iwasaki	0.74092360(2)	6.9016820(2)	-0.29335071(4)
DBW2	-0.0094234(5)	4.0385802(2)	-0.35869680(4)

TABLE VIII: The coefficients $\varepsilon_S^{(0,i)}$ (Eq. (29)) for different actions.

Action	$\varepsilon_S^{(1,1)}$	$\varepsilon_S^{(1,2)}$	$\varepsilon_S^{(1,3)}$
Plaquette	0.6586287(1)	-4.20298580(6)	-1.286053869(4)
Symanzik	0.33939970(4)	-3.76353718(6)	-1.150059945(4)
TILW (8.45)	0.1463203(2)	-3.42960982(2)	-1.054472092(1)
TILW (8.00)	0.1155729(2)	-3.36704753(5)	-1.037165442(1)
Iwasaki	-0.05097214(7)	-2.88571027(1)	-0.909503374(3)
DBW2	-0.1248521(3)	-1.15247167(2)	-0.53943631(1)

TABLE IX: The coefficients $\varepsilon_S^{(1,i)}$ (Eq. (29)) for different actions.

Action	$\varepsilon_S^{(2,1)}$	$\varepsilon_S^{(2,2)}$	$\varepsilon_S^{(2,3)}$
Plaquette	2.60041308(7)	-4.15080331(7)	0.17641091(2)
Symanzik	2.3547298(2)	-3.85277871(9)	0.196461884(5)
TILW (8.45)	2.1881285(8)	-3.6249313(5)	0.21113016(1)
TILW (8.00)	2.1605653(8)	-3.58171175(4)	0.21385016(2)
Iwasaki	2.02123300(8)	-3.23459547(4)	0.234502732(7)
DBW2	2.3731619(3)	-1.9332087(1)	0.2953480(3)

TABLE X: The coefficients $\varepsilon_S^{(2,i)}$ (Eq. (29)) for different actions.

Action	$\varepsilon_P^{(0,1)}$	$\varepsilon_P^{(0,2)}$	$\varepsilon_P^{(2,1)}$	$\varepsilon_P^{(2,2)}$
Plaquette	9.95102761(8)	3.43328275(3)	0.84419938(7)	-0.25823485(3)
Symanzik	8.7100837(1)	2.98705498(3)	0.70640549(6)	-0.27556247(3)
TILW (8.45)	7.84510495(6)	2.67986902(3)	0.65030355(6)	-0.28812231(2)
TILW (8.00)	7.6896423(1)	2.62578350(2)	0.64432843(6)	-0.29027771(3)
Iwasaki	6.55611308(7)	2.25383382(3)	0.66990790(5)	-0.30221183(3)
DBW2	2.9781769(6)	1.24882665(4)	1.5569125(1)	-0.3362271(2)

TABLE XI: The coefficients $\varepsilon_P^{(0,i)}$ and $\varepsilon_P^{(2,i)}$ (Eq. (30)) for different actions.

Action	$\varepsilon_V^{(0,1)}$	$\varepsilon_V^{(0,2)}$	$\varepsilon_V^{(0,3)}$
Plaquette	3.97338480(2)	-2.49669620(4)	0.85409908(1)
Symanzik	3.57961385(3)	-2.21267683(2)	0.77806655(1)
TILW (8.45)	3.32483844(4)	-2.01347343(2)	0.72217154(1)
TILW (8.00)	3.28098129(5)	-1.97788691(3)	0.71193712(2)
Iwasaki	2.98283189(2)	-1.72542048(4)	0.63679613(2)
DBW2	2.25812410(4)	-1.00964505(3)	0.40188086(2)

TABLE XII: The coefficients $\varepsilon_V^{(0,i)}$ (Eq. (31)) for different actions.

Action	$\varepsilon_V^{(1,1)}$	$\varepsilon_V^{(1,2)}$	$\varepsilon_V^{(1,3)}$
Plaquette	2.7109817(1)	-1.84813992(2)	-0.39052850(2)
Symanzik	2.09743725(3)	-1.51877201(8)	-0.385127257(2)
TILW (8.45)	1.64290440(2)	-1.2579161(2)	-0.37793187(2)
TILW (8.00)	1.55841933(4)	-1.20780827(3)	-0.3761606511(4)
Iwasaki	0.9074321(1)	-0.80352187(4)	-0.356005234(3)
DBW2	-1.4498098(4)	0.8826550(3)	-0.264655885(7)

TABLE XIII: The coefficients $\varepsilon_V^{(1,i)}$ (Eq. (31)) for different actions.

Action	$\varepsilon_V^{(2,1)}$	$\varepsilon_V^{(2,2)}$	$\varepsilon_V^{(2,3)}$
Plaquette	1.5541024(2)	0.32907377(4)	-0.0060202576(6)
Symanzik	1.6762868(2)	0.22601986(5)	0.02822949(2)
TILW (8.45)	1.63378530(3)	0.16772628(3)	0.04300929(5)
TILW (8.00)	1.6190247(1)	0.15805313(3)	0.04550457(5)
Iwasaki	1.4573118(1)	0.0858961(2)	0.07934994(2)
DBW2	-1.1604825(4)	-0.0504803(3)	0.13992474(3)

TABLE XIV: The coefficients $\varepsilon_V^{(2,1)} - \varepsilon_V^{(2,3)}$ (Eq. (31)) for different actions.

Action	$\varepsilon_V^{(2,4)}$	$\varepsilon_V^{(2,5)}$	$\varepsilon_V^{(2,6)}$
Plaquette	0.2500659(2)	0.8859920(1)	-0.300364436(2)
Symanzik	0.0214112(1)	0.8342659(2)	-0.28736163(1)
TILW (8.45)	-0.1100958(1)	0.791026749(4)	-0.27444757(3)
TILW (8.00)	-0.1318272(2)	0.78255494(3)	-0.27181092(1)
Iwasaki	-0.2668492(1)	0.712786719(6)	-0.25078366(2)
DBW2	-0.1528741(6)	0.42190739(4)	-0.13978037(7)

TABLE XV: The coefficients $\varepsilon_V^{(2,4)} - \varepsilon_V^{(2,6)}$ (Eq. (31)) for different actions.

Action	$\varepsilon_V^{(2,7)}$	$\varepsilon_V^{(2,8)}$	$\varepsilon_V^{(2,9)}$
Plaquette	1.27887765(9)	0.27776135(2)	-0.35475044(2)
Symanzik	1.03773908(9)	0.28969451(4)	-0.302816648(5)
TILW (8.45)	0.89400856(7)	0.2930984(2)	-0.25886703(3)
TILW (8.00)	0.87034685(8)	0.29343883(9)	-0.25031691(5)
Iwasaki	0.76263373(2)	0.29755270(5)	-0.184270928(8)
DBW2	1.7371355(5)	0.2960594(1)	0.10831780(4)

TABLE XVI: The coefficients $\varepsilon_V^{(2,7)} - \varepsilon_V^{(2,9)}$ (Eq. (31)) for different actions.

Action	$\varepsilon_A^{(0,1)}$	$\varepsilon_A^{(1,1)}$	$\varepsilon_A^{(1,2)}$	$\varepsilon_A^{(1,3)}$
Plaquette	-0.84813073(8)	1.34274645(8)	-1.71809242(4)	0.130176166(7)
Symanzik	-0.48369852(8)	0.92541220(1)	-1.54604828(4)	0.128375752(4)
TILW (8.45)	-0.2452231(1)	0.64518173(2)	-1.42093097(4)	0.125977289(1)
TILW (8.00)	-0.20406156(8)	0.59652190(3)	-1.39831769(4)	0.125386884(3)
Iwasaki	0.0752372(1)	0.2684958(1)	-1.238019617(7)	0.1186684108(9)
DBW2	0.7643240(1)	-0.56650487(5)	-0.75581589(7)	0.088218628(3)

TABLE XVII: The coefficients $\varepsilon_A^{(0,1)}$ and $\varepsilon_A^{(1,i)}$ (Eq. (32)) for different actions.

Action	$\varepsilon_A^{(2,1)}$	$\varepsilon_A^{(2,2)}$	$\varepsilon_A^{(2,3)}$
Plaquette	0.3879068(1)	1.85116980(8)	-0.093094486(8)
Symanzik	0.29616583(7)	1.7629637(2)	-0.11136345(3)
TILW (8.45)	0.2483248(2)	1.65782471(1)	-0.118658311(8)
TILW (8.00)	0.2378781(2)	1.63840648(4)	-0.11982438(1)
Iwasaki	0.05917686(4)	1.5707047(2)	-0.13932655(1)
DBW2	-2.2341918(4)	1.22932319(6)	-0.17119304(8)

TABLE XVIII: The coefficients $\varepsilon_A^{(2,1)} - \varepsilon_A^{(2,3)}$ (Eq. (32)) for different actions.

Action	$\varepsilon_A^{(2,4)}$	$\varepsilon_A^{(2,5)}$	$\varepsilon_A^{(2,6)}$
Plaquette	1.6350438(1)	-1.59945524(6)	0.333900263(8)
Symanzik	1.3008790(1)	-1.48761993(3)	0.314172576(5)
TILW (8.45)	1.0461303(2)	-1.39361896(4)	0.297787700(5)
TILW (8.00)	0.9998744(1)	-1.37577372(4)	0.29455820(2)
Iwasaki	0.6845753(1)	-1.24800562(3)	0.26827353(2)
DBW2	0.0967251(2)	-0.735419342(8)	0.14738921(4)

TABLE XIX: The coefficients $\varepsilon_A^{(2,4)} - \varepsilon_A^{(2,6)}$ (Eq. (32)) for different actions.

Action	$\varepsilon_A^{(2,7)}$	$\varepsilon_A^{(2,8)}$	$\varepsilon_A^{(2,9)}$
Plaquette	0.41758917(4)	0.395847810(9)	0.31972188(2)
Symanzik	0.596637529(2)	0.33473715(4)	0.27870681(2)
TILW (8.45)	0.73021636(8)	0.29171961(4)	0.24115534(2)
TILW (8.00)	0.75716237(6)	0.28297665(3)	0.233647603(8)
Iwasaki	1.05772129(4)	0.18672220(2)	0.17428813(3)
DBW2	3.4449465(4)	-0.22085461(4)	-0.10748502(5)

TABLE XX: The coefficients $\varepsilon_A^{(2,7)} - \varepsilon_A^{(2,9)}$ (Eq. (32)) for different actions.

Action	$\varepsilon_T^{(0,1)}$	$\varepsilon_T^{(0,2)}$	$\varepsilon_T^{(0,3)}$
Plaquette	0.37366536(7)	-1.66446414(3)	-0.5750281973(1)
Symanzik	0.51501972(4)	-1.47511786(3)	-0.4769739579(4)
TILW (8.45)	0.62806240(5)	-1.34231565(2)	-0.411841977(2)
TILW (8.00)	0.64974666(4)	-1.31859128(1)	-0.4006364262(1)
Iwasaki	0.82253993(3)	-1.15028034(3)	-0.3267471901(5)
DBW2	1.5201736(4)	-0.67309671(3)	-0.1483549734(1)

TABLE XXI: The coefficients $\varepsilon_T^{(0,i)}$ (Eq. (34)) for different actions.

Action	$\varepsilon_T^{(1,1)}$	$\varepsilon_T^{(1,2)}$	$\varepsilon_T^{(1,3)}$
Plaquette	-4.05372833(7)	1.866287582(5)	-0.8573692476(6)
Symanzik	-3.0228493(1)	1.59558642(1)	-0.7667066321(8)
TILW (8.45)	-2.28808611(8)	1.39406610(3)	-0.7029813946(7)
TILW (8.00)	-2.15494125(2)	1.357142525(7)	-0.691443627(2)
Iwasaki	-1.17592792(3)	1.087913642(4)	-0.6063355831(7)
DBW2	2.0163147(3)	0.15488056(9)	-0.359624204(3)

TABLE XXII: The coefficients $\varepsilon_T^{(1,i)}$ (Eq. (34)) for different actions.

Action	$\varepsilon_T^{(2,1)}$	$\varepsilon_T^{(2,2)}$	$\varepsilon_T^{(2,3)}$
Plaquette	2.3328621(2)	-1.52209604(8)	0.23683195(1)
Symanzik	2.4912319(2)	-1.53694399(3)	0.26295051(2)
TILW (8.45)	2.4578347(1)	-1.49009843(6)	0.26767225(1)
TILW (8.00)	2.44550431(4)	-1.48035333(8)	0.26834751(3)
Iwasaki	2.3441345(2)	-1.4848088(1)	0.30172406(2)
DBW2	1.3013094(2)	-1.2798033(3)	0.3475909(1)

TABLE XXIII: The coefficients $\varepsilon_T^{(2,1)} - \varepsilon_T^{(2,3)}$ (Eq. (34)) for different actions.

Action	$\varepsilon_T^{(2,4)}$	$\varepsilon_T^{(2,5)}$	$\varepsilon_T^{(2,6)}$
Plaquette	-2.02795509(9)	0.11808647(1)	0.07250824(3)
Symanzik	-1.55221265(9)	0.04504264(4)	0.07020813(1)
TILW (8.45)	-1.2361662(1)	-0.00137858(3)	0.06309676(1)
TILW (8.00)	-1.17754207(2)	-0.0104623(1)	0.06169762(2)
Iwasaki	-0.6509124(1)	-0.11083048(4)	0.06071268(8)
DBW2	1.4802111(2)	-0.51691409(6)	0.03446776(7)

TABLE XXIV: The coefficients $\varepsilon_T^{(2,4)} - \varepsilon_T^{(2,6)}$ (Eq. (34)) for different actions.

Action	$\varepsilon_T^{(2,7)}$	$\varepsilon_T^{(2,8)}$	$\varepsilon_T^{(2,9)}$
Plaquette	0.3932905(2)	1.10184617(6)	-0.02744360(1)
Symanzik	0.1467998(1)	1.03762644(2)	-0.03500219(3)
TILW (8.45)	-0.0094312(1)	0.97633518(7)	-0.038311849(6)
TILW (8.00)	-0.0364177(1)	0.96442476(2)	-0.03892456(3)
Iwasaki	-0.2049940(1)	0.88259379(5)	-0.04896801(2)
DBW2	-0.3118850(6)	0.51292384(2)	-0.07146761(1)

TABLE XXV: The coefficients $\varepsilon_T^{(2,7)} - \varepsilon_T^{(2,9)}$ (Eq. (34)) for different actions.

Action	$\varepsilon_{T'}^{(2,1)}$	$\varepsilon_{T'}^{(2,4)}$	$\varepsilon_{T'}^{(2,7)}$
Plaquette	0.00047095(5)	-0.30537822(7)	1.4070324(1)
Symanzik	-0.26900984(7)	-0.67000961(5)	1.0574111(1)
TILW (8.45)	-0.31308657(6)	-0.90858179(3)	0.7651952(1)
TILW (8.00)	-0.31678921(7)	-0.95117312(1)	0.7107479(2)
Iwasaki	-0.45213470(9)	-1.24108756(9)	0.3465297(2)
DBW2	-0.8461093(2)	-1.9354110(1)	-0.6289363(3)

TABLE XXVI: The coefficients $\varepsilon_{T'}^{(2,1)}, \varepsilon_{T'}^{(2,4)}, \varepsilon_{T'}^{(2,7)}$ (Eq. (35)) for different actions.

Action	$\varepsilon_{T'}^{(2,8)}$	$\varepsilon_{T'}^{(2,9)}$
Plaquette	0.28175492(1)	0.054718244(7)
Symanzik	0.24663315(4)	0.06136902(2)
TILW (8.45)	0.2319752(1)	0.06397589(2)
TILW (8.00)	0.22947913(7)	0.064400395(7)
Iwasaki	0.19560470(5)	0.07153771(1)
DBW2	0.13147908(9)	0.08509400(2)

TABLE XXVII: The coefficients $\varepsilon_{T'}^{(2,8)}, \varepsilon_{T'}^{(2,9)}$ (Eq. (35)) for different actions.